

Brownian dynamics with hydrodynamic interactions

Donald L. Ermak and J. A. McCammon

Citation: *J. Chem. Phys.* **69**, 1352 (1978); doi: 10.1063/1.436761

View online: <http://dx.doi.org/10.1063/1.436761>

View Table of Contents: <http://jcp.aip.org/resource/1/JCPSA6/v69/i4>

Published by the [American Institute of Physics](#).

Additional information on J. Chem. Phys.

Journal Homepage: <http://jcp.aip.org/>

Journal Information: http://jcp.aip.org/about/about_the_journal

Top downloads: http://jcp.aip.org/features/most_downloaded

Information for Authors: <http://jcp.aip.org/authors>

ADVERTISEMENT



AIPAdvances

Special Topic Section:
PHYSICS OF CANCER

Why cancer? Why physics? [View Articles Now](#)

Brownian dynamics with hydrodynamic interactions

Donald L. Ermak

Biomedical and Environmental Research Division, Lawrence Livermore Laboratory, University of California, Livermore, California 94550

J. A. McCammon

Department of Chemistry, Harvard University, Cambridge, Massachusetts 02138

(Received 9 February 1978)

A method for simulating the Brownian dynamics of N particles with the inclusion of hydrodynamic interactions is described. The particles may also be subject to the usual interparticle or external forces (e.g., electrostatic) which have been included in previous methods for simulating Brownian dynamics of particles in the absence of hydrodynamic interactions. The present method is derived from the Langevin equations for the N particle assembly, and the results are shown to be consistent with the corresponding Fokker-Planck results. Sample calculations on small systems illustrate the importance of including hydrodynamic interactions in Brownian dynamics simulations. The method should be useful for simulation studies of diffusion limited reactions, polymer dynamics, protein folding, particle coagulation, and other phenomena in solution.

I. INTRODUCTION

In this paper we present a method for simulating the diffusive behavior of a system of N interacting Brownian particles in solution. The effects of hydrodynamic interactions mediated by the host solvent are included through a position-dependent interparticle friction tensor. As presented here, the simulation technique is applicable to spherically symmetric Brownian particles and particles composed of spherically symmetric sub-units.

The theory of Brownian motion was developed to describe the dynamic behavior of particles whose mass and size are much larger than those of the host medium particles. It has been applied to dilute solutions of large molecules and colloidal particles. Two approaches have generally been used. One is based on the Fokker-Planck differential equation for the time evolution of the N particle phase space distribution function $W(\{r_i\}, \{p_i\}, t)$. The other approach uses $3N$ coupled Langevin equations to describe the motion of the N particles.

While the two approaches are different, they are equivalent in that the statistical description of the N particle phase space trajectories are identical with both methods. Solution of the Fokker-Planck equation yields directly the phase space distribution function $W(\{r_i\}, \{p_i\}, t)$. On the other hand, with the set of coupled Langevin equations, one can directly calculate N particle phase space trajectories and then obtain $W(\{r_i\}, \{p_i\}, t)$ by averaging.

The theory of Brownian motion originated with the works of Einstein,¹ Smoluchowski,^{2,3} Langevin,⁴ Fokker,^{5,6} and Planck.⁷ Since their early works the theory has been developed and applied by numerous authors in the study of a single Brownian particle in solution.⁸⁻¹⁵ The two-particle Fokker-Planck equation was first derived by Mazo.¹⁶ Subsequently, Deutch and Oppenheim derived a generalized Langevin equation from the Liouville equation for N Brownian particles and n fluid particles; and from the Langevin equation they derived the N particle Fokker-Planck equation.¹⁷

Due to the large mass and size of the Brownian particles, the distribution of momenta relaxes to the equilibrium distribution much more rapidly than does the distribution of particle positions. Physically, this occurs as a result of the many collisions which the Brownian particle has with the surrounding fluid particles. The distribution of momenta essentially reaches the equilibrium distribution before the positions of the Brownian particles have changed significantly when compared to the average distance between the Brownian particles or (for sufficiently large particles) the diameter of the Brownian particles. Consequently, for many applications of the theory, one is concerned only with phenomena which occur on a time scale which is much larger than the momentum relaxation time. We shall refer to times on this time scale as the diffusion regime. In this case one is concerned only with the time evolution of the N particle configuration space distribution function and the particle momenta are characterized simply by their equilibrium distribution function.

Derivation of the N particle configuration space Fokker-Planck equation in the diffusion regime was achieved by Murphy and Aguirre¹⁸ by integrating the phase space Fokker-Planck equation over the particle momenta and expanding the resultant distribution function in a power series. The particle position Langevin equations which correspond to the configuration space Fokker-Planck equation have been presented by Lax¹⁹ and Zwanzig.²⁰ Here we derive the set of particle position Langevin equations directly from the particle momentum Langevin equations and present a method for numerically simulating the configuration space equations of motion in a computer experiment.

In the following section the Fokker-Planck formalism is briefly reviewed and the mean particle displacement and square displacement are calculated. Next we derive the particle position Langevin equations from the particle momentum equations by making use of the assumption of rapid momentum relaxation. Then the simulation technique is presented using the Oseen tensor²¹ and the Rotne-Prager tensor²² approximations for

the hydrodynamic interaction mediated by the fluid. In Sec. V the simulation technique is illustrated by computer experiments on dimer and trimer particle systems.

II. FOKKER-PLANCK DESCRIPTION

The system under consideration consists of N Brownian particles immersed in a viscous, incompressible solvent continuum. The particles may be subject to configuration-dependent forces due to interparticle interactions (e.g., electrostatic coupling) or external fields (e.g., gravitational fields). The particles are also subject to velocity-dependent hydrodynamic interactions; here these are treated within the approximation of pairwise additivity by use of a configuration-dependent friction tensor ζ_{ij} . The Fokker-Planck equation used to describe this system is^{18,23}

$$\frac{\partial W}{\partial t} + \sum_i \left(m_i^{-1} p_i \frac{\partial W}{\partial r_i} + F_i \frac{\partial W}{\partial p_i} \right) = \sum_i \sum_j \frac{\partial}{\partial p_i} \zeta_{ij} \left(m_j^{-1} p_j W + kT \frac{\partial W}{\partial p_j} \right), \quad (1)$$

where i and j run over the particle coordinates ($1 \leq i, j \leq 3N$), F_i is the sum of interparticle and external forces acting in direction i , m_i is the mass of the particle associated with index i , r_i and p_i are position and momentum components, respectively, k is Boltzmann's constant, and T is the absolute temperature. The N particle phase-space distribution function $W(\{r_i\}, \{p_i\}, t)$ is the average number density of Brownian particles at $\{r_i\}, \{p_i\}$ at time t which evolves from the initial distribution $W(\{r_i\}, \{p_i\}, 0)$.

Using a method of the Chapman-Enskog type, Murphy and Aguirre¹⁸ derive from Eq. (1) the diffusion equation for the N particle system

$$\frac{\partial W}{\partial t} = \sum_i \sum_j \frac{\partial}{\partial r_i} D_{ij} \left(\frac{\partial W}{\partial r_j} - \frac{1}{kT} F_j W \right), \quad (2)$$

where $W(\{r_i\}, t)$ is the N particle configuration space distribution function and $D_{ij} = D_{ji}$ is the (configuration-dependent) diffusion tensor related to ζ_{ij} by

$$\sum_j \zeta_{ij} D_{ji} = \sum_j D_{ij} \zeta_{ji} = kT \delta_{ii}. \quad (3)$$

This reduction has also been achieved by Wilemski.²³ In arriving at Eq. (2) it was assumed that the momentum variables relax to equilibrium much more rapidly than the position variables and that all spatial gradients, including the force F_j , are reasonably smooth functions of the particle configurations.¹⁸ In accordance with these assumptions, Eq. (2) is valid only for time intervals $\Delta t \gg m_i/\zeta_{ii}$, the velocities $\{v_i(t + \Delta t)\}$ are effectively uncorrelated with the velocities $\{v_i(t)\}$, and the mean square velocity component of each Brownian particle over time intervals $\gtrsim \Delta t$ is the equilibrium value $\langle v_i^2 \rangle = kT/m_i$.

In computer experiments one is concerned with calculating the particle displacements over short time steps Δt . To minimize the number of time steps required to calculate a trajectory Δt is chosen as large as possible subject to the requirement that the forces

on the particles remain nearly constant during each step. In Brownian dynamics methods the particle displacements are chosen according to stochastic rules.²⁴ The successive configurations of a Brownian trajectory are selected from the configuration space distribution function $W(\{r_i\}, t)$. In such a procedure the Brownian particle positions are known ($\{r_i^0\}$) at the start of a given step ($\Delta t = 0$) and the corresponding initial distribution function is $W(\{r_i^0\}, 0) = \prod \delta(r_i - r_i^0)$, where $\delta(r)$ is the Dirac delta function. Then, to first order in Δt , the solution to Eq. (2) is the multivariate Gaussian distribution function $W(\{r_i\}, \Delta t)$ which is uniquely defined by the moments

$$\langle \Delta r_i(\Delta t) \rangle = \sum_j \left(\frac{\partial D_{ij}}{\partial r_j} + \frac{D_{ij}}{kT} F_j \right) \Delta t \quad (4a)$$

and

$$\langle \Delta r_i(\Delta t) \Delta r_j(\Delta t) \rangle = 2D_{ij}\Delta t, \quad (4b)$$

where the diffusion tensor, the gradient of the diffusion tensor, and the forces are all evaluated in the initial configuration ($\Delta t = 0$). The configuration of the system at the end of the step is chosen from $W(\{r_i\}, \Delta t)$ and the procedure is repeated to develop one typical Brownian trajectory.

The hydrodynamic interaction between the Brownian particles affects both the mean and the covariance of the particle displacements. In the absence of hydrodynamic interactions the diffusion tensor is diagonal and constant, so that Eq. (4) becomes

$$\langle \Delta r_i(\Delta t) \rangle = \frac{D_{ii}}{kT} F_i \Delta t, \quad (5a)$$

$$\langle \Delta r_i(\Delta t) \Delta r_j(\Delta t) \rangle = 2D_{ii}\Delta t \delta_{ij}. \quad (5b)$$

In this case the average displacement of a particle is proportional to the force on that particle only, while in the presence of hydrodynamic interactions the average displacement is composed of two terms, one proportional to the gradient of the diffusion tensor and the other proportional to a weighted sum of the forces acting on all the Brownian particles. The presence of hydrodynamic interaction also leads to cross correlations in the displacements of different particles, but does not alter the mean square displacements $\langle [\Delta r_i(\Delta t)]^2 \rangle$.¹⁷

III. LANGEVIN DESCRIPTION

Traditional deterministic molecular dynamics calculations begin with an equation of motion for the particles and calculate the displacements over successive time intervals Δt by integrating these equations. In this section we develop the parallel approach for the Brownian dynamics of particles with hydrodynamic interactions.

The Langevin equations for the system of N Brownian particles described in the previous section are¹⁷

$$m_i \dot{v}_i = - \sum_j \zeta_{ij} v_j + F_i + \sum_j \alpha_{ij} f_j. \quad (6)$$

Equation (6) is an expression of Newton's law, equating the change in momenta $\dot{p}_i = m_i \dot{v}_i$ to the forces which act on the Brownian particles. The indices i and j label components ($1 \leq i, j \leq 3N$) and $\sum_j \alpha_{ij} f_j$ represents the

randomly fluctuating force exerted on a particle by the surrounding fluid. The f_j are described by a Gaussian distribution with the mean and covariance

$$\langle f_i \rangle = 0, \quad (7a)$$

$$\langle f_i(t) f_j(t') \rangle = 2\delta_{ij} \delta(t - t'). \quad (7b)$$

The coefficients α_{ij} are related to the hydrodynamic friction tensor by

$$\zeta_{ij} = \frac{1}{kT} \sum_l \alpha_{il} \alpha_{jl}. \quad (7c)$$

The force on each Brownian particle is therefore composed of three terms: a friction force which tends to decrease the particle energy, a random force which tends to increase the particle energy, and a systematic force due to the interaction potential energy between Brownian particles plus any external force.

We seek an equation for the displacements of the Brownian particle starting from the momentum Langevin equation [Eq. (6)]. As in the preceding section, we will assume that the time scales for momentum relaxation and position relaxation of the Brownian particles are well separated. Then it is possible to consider only time intervals longer than the momentum relaxation times; the displacement equation corresponding to this diffusive regime will be referred to as the diffusive displacement equation.

The first step in deriving the diffusive displacement equation is to express Eq. (6) in a slightly different form by using the diffusion tensor defined in Eq. (3). Multiplying Eq. (6) by D_{ii}/kT , summing over i , and changing dummy indices yields

$$\sum_j \tau_{ij} \dot{v}_j = -v_i + \frac{1}{kT} \sum_j D_{ij} F_j + \sum_j \sigma_{ij} f_j \quad (8)$$

where

$$\tau_{ij} \equiv D_{ij} m_j / kT$$

and

$$\sigma_{ij} = \frac{1}{kT} \sum_l D_{il} \alpha_{lj}.$$

From Eq. (7c) it follows that

$$D_{ij} = \sum_l \sigma_{il} \sigma_{jl}.$$

Expanding τ_{ij} in a Taylor series about the initial positions of the Brownian particles yields

$$\tau_{ij} = \tau_{ij}^0 + \sum_l \frac{\partial \tau_{ij}^0}{\partial r_l} \Delta r_l + \dots,$$

where $\Delta r_l = r_l(t) - r_l(0)$ and the superscript indicates that the $t=0$ value is implied. Corresponding expansions may be written for D_{ij} , σ_{ij} , and F_j ; in the pairwise interaction approximation the coefficients of Δr_l vanish in all these expansions if l is associated with different particles than i and j are. To calculate the means and covariances of the particle displacements to first order in Δt it will only be necessary to retain the first order terms in τ_{ij} and the zeroth order terms in D_{ij} , σ_{ij} , and F_j .

Substituting these expansions into Eq. (8), separating out the terms involving v_i and \dot{v}_i , and retaining only terms of the orders indicated above yields

$$\begin{aligned} \tau_{ii}^0 \dot{v}_i + v_i &= \tau_{ii}^0 \exp(-t/\tau_{ii}^0) \frac{d}{dt} [\exp(t/\tau_{ii}^0) v_i] \\ &= - \sum_j' \tau_{ij}^0 \dot{v}_j - \sum_j \sum_l \frac{\partial \tau_{ij}^0}{\partial r_l} \Delta r_l \dot{v}_j \\ &\quad + \frac{1}{kT} \sum_j D_{ij}^0 F_j^0 + \sum_j \sigma_{ij}^0 f_j, \end{aligned} \quad (9)$$

where the prime on the summation indicates that the $j=i$ term is omitted.

An equation for $v_i(t)$ can be obtained by multiplying Eq. (9) by $(\tau_{ii}^0)^{-1} \exp(t/\tau_{ii}^0)$ and integrating over time. A second integration over time yields an equation for the displacement of the Brownian particle $\Delta r_i(t)$. The double integral over time in the displacement equation can be removed by an integration by parts and the result is

$$\begin{aligned} \Delta r_i(t) &= \tau_{ii}^0 v_i(0) [1 - \exp(-t/\tau_{ii}^0)] - \sum_j' \tau_{ij}^0 \int_0^t ds [1 - \exp(-(t-s)/\tau_{ii}^0)] \dot{v}_j \\ &\quad + \sum_j \int_0^t ds \{1 - \exp[-(t-s)/\tau_{ii}^0]\} \left(- \sum_l \frac{\partial \tau_{ij}^0}{\partial r_l} \Delta r_l \dot{v}_j + \sigma_{ij}^0 f_j + \frac{D_{ij}^0}{kT} F_j^0 \right). \end{aligned} \quad (10)$$

Equation (10) can be simplified by restricting the time step t to times such that $t \gg \tau_{ii}^0 \equiv m_i D_{ii}^0 / kT$. In this time regime the exponential coefficient $\exp(-t/\tau_{ii}^0) \approx 0$ and the coefficient $1 - \exp[-(t-s)/\tau_{ii}^0] \approx 1$ on the interval $0 \leq s < t$. When $s=t$, this coefficient is zero. Noting that v is on the order of $(kT/m)^{1/2}$ and Δr is on the order of $(Dt)^{1/2}$, it follows that $t^2 v \sim (m/kT)^{1/2} D \ll (Dt)^{1/2} \sim \Delta r$. Therefore, neglecting the $\tau^0 v$ terms in Eq. (10) and using the approximation discussed above, Eq. (10) becomes

$$\begin{aligned} \Delta r_i &= \sum_j \left(- \sum_l \frac{\partial \tau_{ij}^0}{\partial r_l} \int_0^t ds \Delta r_l \dot{v}_j + \frac{D_{ij}^0}{kT} F_j^0 t \right) \\ &\quad + \sum_j \sigma_{ij}^0 \int_0^t ds \{1 - \exp[-(t-s)/\tau_{ii}^0]\} f_j(s). \end{aligned} \quad (11)$$

The exponential coefficient has been retained in the random force term as its value at $s=t$ is essential to the proper evaluation of the average of this term.

The terms in $\Delta r \dot{v}$ can be put in a more useful form by noting that

$$\Delta r_i \dot{v}_j = \frac{d}{dt} (\Delta r_i v_j) - v_i v_j.$$

Integrating this equation over time and using the approximation

$$\int_0^t ds v_i v_j \approx \frac{kT}{m_i} t \delta_{ij}$$

for $t \gg \tau_{ii}^0$, one obtains

$$\int_0^t ds \Delta r_i \dot{v}_j \approx \Delta r_i v_j - \frac{kT}{m_i} t \delta_{ij}.$$

Again, for $t \gg \tau_{ii}^0$, the first term on the rhs can be neglected since $\Delta r v \approx [(kTD/m)t]^{1/2} \ll (kT/m)t$. With this result Eq. (11) can be simplified to

$$\Delta r_i = \sum_j \frac{\partial D_{ij}^0}{\partial r_j} t + \sum_j \frac{D_{ij}^0 F_j^0}{kT} t + \sum_j \int_0^t ds \{1 - \exp[-(t-s)/\tau_{ij}^0]\} \sigma_{ij}^0 f_j(s). \quad (12)$$

In the expansion of σ only the first term was retained since higher order terms do not contribute to $\langle \Delta r_i \rangle$ or $\langle \Delta r_i \Delta r_j \rangle$ to first order in t . This can readily be seen by evaluating $\langle \Delta r_i(t) f_j(t) \rangle$. Using Eq. (12) for Δr_i and dropping terms of order $sf(s)$ and $\Delta r^2(s)f(s)$, we obtain

$$\begin{aligned} \langle \Delta r_i(t) f_j(t) \rangle &= \sum_i \int_0^t ds \{1 - \exp[-(t-s)/\tau_{ii}^0]\} \sigma_{ii}^0 \langle f_i(s) f_j(t) \rangle \\ &= 2 \int_0^t ds \{1 - \exp[-(t-s)/\tau_{ii}^0]\} \sigma_{ii}^0 \delta(s-t) = 0. \end{aligned} \quad (13)$$

The mean displacement is readily calculated from Eq. (12) and is

$$\langle \Delta r_i \rangle = \sum_j \left(\frac{\partial D_{ij}^0}{\partial r_j} + \frac{D_{ij}^0 F_j^0}{kT} \right) t. \quad (14a)$$

The covariance of the displacements is, to first order in t ,

$$\begin{aligned} \langle \Delta r_i \Delta r_j \rangle &= 2 \sum_i \int_0^t ds \{1 - \exp[-(t-s)/\tau_{ii}^0]\} \\ &\quad \times \{1 - \exp[-(t-s)/\tau_{jj}^0]\} \sigma_{ii}^0 \sigma_{jj}^0 \\ &\approx 2D_{ij}^0 t. \end{aligned} \quad (14b)$$

These results are seen to be in agreement with those of Eq. (4) obtained from the diffusive Fokker-Planck equation [Eq. (2)]. Throughout the above derivation it has been indicated that the minimum time step t is much greater than the momentum relaxation time, i.e., $t \gg \tau^0 = mD/kT$. We have also implicitly assumed in writing Eq. (9) and subsequent equations that t is sufficiently small that ∇D and F are essentially constant during t . It should also be noted that the results given in Eq. (4) or (14) can also be derived by integrating the position Langevin equation given by Zwanzig²⁰ (see also Lax¹⁹).

IV. SIMULATION TECHNIQUE

The general method of Brownian dynamics was outlined in the latter part of Sec. II. The system of Brownian particles is placed in an initial configuration and

then each particle is mathematically moved along a trajectory in accordance with the configuration space distribution function $W(\{r_i\}, t)$ defined by Eq. (2). As the particles move through configuration space their properties (e.g., potential energy, squared displacement, etc.) are calculated and at the end of the simulation the average value of each property during the experiment is obtained. In general, the calculated averages will more closely approach the true system averages as the simulation is run for longer times t .

In a Brownian dynamics computer simulation the configuration space trajectories are calculated numerically, i.e., the trajectories are composed of successive displacements each taken over a short time step Δt . These displacements are to be randomly chosen in accordance with the multivariate Gaussian distribution function $W(\{r_i\}, \Delta t)$ whose moments are specified by Eqs. (4a) and (4b). What is needed is an equation of motion from which the displacements can be calculated.

Such a displacement equation is given by Eq. (12) and can be written more concisely as

$$r_i = r_i^0 + \sum_j \frac{\partial D_{ij}^0}{\partial r_j} \Delta t + \sum_j \frac{D_{ij}^0 F_j^0}{kT} \Delta t + R_i(\Delta t), \quad (15)$$

where the superscript "0" indicates that the variable is to be evaluated at the beginning of the time step. As previously discussed, the size of the physically meaningful time step is restricted to values which are sufficiently long so that $\Delta t \gg m_i D_{ii}^0 / kT$. Numerical accuracy limits the maximum size of the time step, requiring it to be sufficiently short so that the force on the particles and the gradient of the diffusion tensor are essentially constant during Δt . The displacement $R_i(\Delta t)$ is a random displacement with a Gaussian distribution function whose average value is zero and whose variance-covariance is $\langle R_i(\Delta t) R_j(\Delta t) \rangle = 2D_{ij}^0 \Delta t$.

Values for the set of $3N$ displacements $\{R_i\}$ can be obtained from a multivariate normal deviate generator such as the GGNRM subroutine listed in the IMSL Library.²⁵ They may also be calculated from a weighted sum of normal random deviates $\{x_i\}$; $\langle x_i \rangle = 0$, $\langle x_i x_j \rangle = 2\delta_{ij} \Delta t$, where δ_{ij} is the Kronecker delta. Defining the Brownian displacement as

$$R_i(\Delta t) = \sum_{j=1}^i \sigma_{ij} X_j, \quad (16)$$

then the weighting factors are given by

$$\begin{aligned} \sigma_{ii} &= \left(D_{ii} - \sum_{k=1}^{i-1} \sigma_{ik}^2 \right)^{1/2}, \\ \sigma_{ij} &= \left(D_{ij} - \sum_{k=1}^{j-1} \sigma_{ik} \sigma_{jk} \right) / \sigma_{jj}, \quad i > j. \end{aligned} \quad (17)$$

Two diffusion tensors are suggested as approximations to the hydrodynamic interaction mediated by the fluid. The Oseen tensor²¹ given by

$$\begin{aligned} D_{ij} &= \frac{kT}{6\pi\eta a} \delta_{ij}, \quad i, j \text{ on the same particle,} \\ D_{ij} &= \frac{kT}{8\pi\eta r_{ij}} \left(\bar{I} + \frac{\bar{r}_{ij} \bar{r}_{ij}}{r_{ij}^2} \right), \quad i, j \text{ on different particles,} \end{aligned} \quad (18)$$

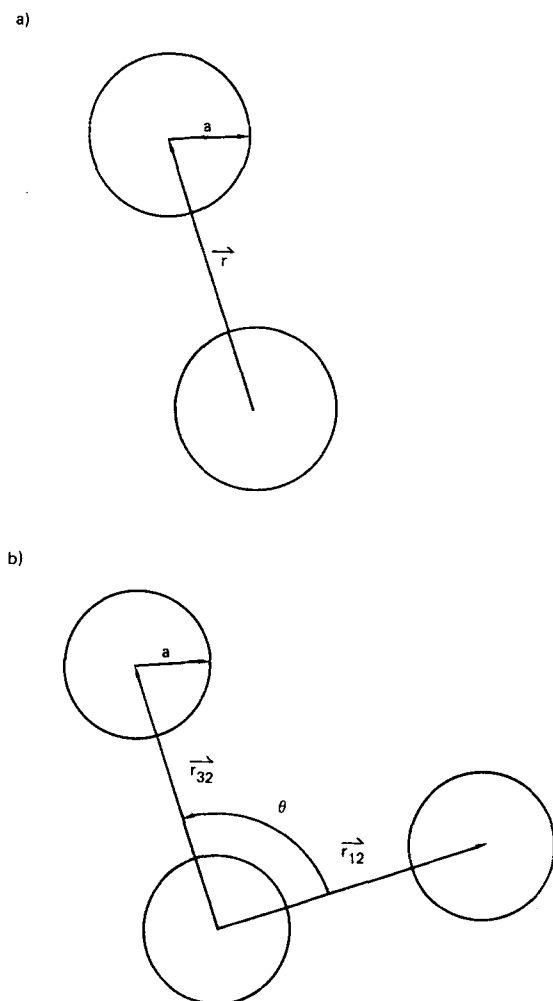


FIG. 1. Conceptual drawing of the (a) dimer and (b) trimer systems.

and the Rotne-Prager tensor²² given by

$$D_{ij} = \frac{kT}{6\pi\eta a} \delta_{ij}, \quad i, j \text{ on the same particle,}$$

$$D_{ij} = \frac{kT}{8\pi\eta r_{ij}} \left[\left(\frac{1}{r_{ij}^2} + \frac{\bar{r}_{ij} \bar{r}_{ij}}{r_{ij}^4} \right) + \frac{2a^2}{r_{ij}^2} \left(\frac{1}{3} \frac{1}{r_{ij}^2} - \frac{\bar{r}_{ij} \bar{r}_{ij}}{r_{ij}^4} \right) \right],$$

$i, j \text{ on different particles.} \quad (19)$

Here η is the solvent viscosity, a is the sphere radius, δ_{ij} is the Kronecker delta, \bar{r}_{ij} is the vector from the center of sphere i to the center of sphere j , and \bar{I} is the unit tensor. Both of these tensors have the property

$$\sum_j \frac{\partial D_{ij}}{\partial r_j} = 0, \quad (20)$$

so that this term can be dropped from Eq. (15). This greatly simplifies the calculation of the displacements as the gradient of the diffusion tensor does not have to be calculated.

V. APPLICATION

As a demonstration of the Brownian dynamics technique with hydrodynamic interactions, the method presented in the previous section is applied to a number of simple dimer and trimer systems (Fig. 1). Each sys-

tem is composed of equal size Brownian particle spheres which are held together by a two particle (pair) potential. Some of the properties of these systems can be calculated analytically and these results are compared with the computer simulation results as a test of the accuracy of the method. Each multiunit system is simulated three times using a different approximation of the hydrodynamic interaction in each simulation. The three hydrodynamic tensor approximations are the Oseen tensor [Eq. (18)], the Rotne-Prager tensor [Eq. (19)], and the constant diagonal tensor with no hydrodynamic interaction [Eq. (5)].

Two types of dimer systems were studied; rigid rod dimers, where the separation distance between the two subunit spheres is constant, and harmonic dimers, where the pair potential between the two subunit spheres is

$$\phi(r) = \frac{kT}{2\delta^2} (l - r)^2, \quad (21)$$

and r is the distance between the sphere centers. The harmonic potential of Eq. (21) is also used as the pair potential between adjacent subunits of the trimer systems. Between the two end spheres of the trimer the pair potential

$$\phi(r) = \begin{cases} \frac{kT}{2\delta^2} (l - r)^2, & r \leq l \\ 0, & r \geq l \end{cases} \quad (22)$$

is used.

All of the results are expressed in dimensionless units. Distance is in units of the separation distance l and time is in units of l^2/D_0 , where $D_0 = kT/6\pi\eta a$ is the diffusion coefficient of a single subunit sphere. The diffusion coefficient of the multiunit system is therefore expressed in units of the single sphere diffusion coefficient D_0 .

A. Rigid rod dimer simulations

The rigid rod pair potential $\phi(r)$ is infinite everywhere except at $r=1$ and then it is zero. The pair force is therefore proportional to the Dirac delta function $\delta(1-r)$ and cannot be used directly in Eq. (15). To account for the constraint of constant separation distance the equation of motion is modified and the displacement of the system is conducted in two steps. First, each subunit is displaced according to Eq. (15) with the force set equal to zero. Then, the two subunits are moved along the line connecting their centers until the separation distance is equal to 1 and in such a manner that the center of mass of the system remains unchanged. This simple method of constraining the subunit separation distance works well for the dimer case; however, for larger multiunit chains, a method such as the one proposed by Ryckaert *et al.*²⁶ is probably more useful.

Two properties of the dimer were studied: translational diffusion and the rate of rotation. The translational diffusion coefficient is defined as

$$D = \frac{\langle (\mathbf{r}_c(t) - \mathbf{r}_c(0)) \rangle^2}{6t}, \quad (23)$$

where \mathbf{r}_0 is the dimer center of mass, t is time, and $\langle \rangle$ denotes the average value. Dimer rotation is studied by calculating the average value of

$$\cos\theta(t) = \hat{\mathbf{r}}_0(t) \cdot \hat{\mathbf{r}}_0(0), \quad (24)$$

where $\hat{\mathbf{r}}_0$ is a unit vector from the center of one sphere to the center of the other. The average value of $\cos\theta(t)$ decays exponentially with time and the decay constant is designated as α .

The analytic values of the translational diffusion coefficient D and the rotational decay rate α are readily calculated. The values for each of the hydrodynamic tensor approximations are as follows;

$$\begin{aligned} \text{Oseen tensor:} \quad & D = 0.5(1 + a), \\ & \alpha = 4(1 - 3a/4); \\ \text{Rotne-Prager tensor:} \quad & D = 0.5(1 + a), \quad (25) \\ & \alpha = 4(1 - 3a/4 - a^3/2); \\ \text{No hydrodynamic interaction:} \quad & D = 0.5 \\ & \alpha = 4, \end{aligned}$$

where " a " is the subunit radius in units of l the separation distance.

Computer simulations of six systems were conducted with the radius of the subunit spheres varied from 0.5 (the maximum possible radius) to 0.005. The time step used in the calculations was $\Delta t = 0.00125$ and each simulation was conducted for 10 000 time steps.

The translational diffusion coefficient results are shown in Table I and the rotational decay rate results are shown in Table II. Both the values obtained from the computer simulation and the analytic values are given. The computer results are seen to be in good agreement with the analytic values and the difference is within the statistical error associated with the length of the computer runs.

In the absence of hydrodynamic interaction the translational diffusion coefficient and rotational decay rate are independent of the subunit radius and have the constant values of $D = 0.5$ and $\alpha = 4.0$, respectively. When the subunit radius is very small in comparison to the separation distance, the hydrodynamic interaction as expressed by the Oseen and Rotne-Prager tensors has

TABLE I. Rigid rod dimer diffusion coefficients.

Radius a	Oseen		Rotne-Prager		No hydrodynamic interaction	
	D^a	$D_{\text{calc.}}^b$	D	$D_{\text{calc.}}$	D	$D_{\text{calc.}}$
0.500	0.7500	0.749	0.7500	0.744	0.5000	0.500
0.250	0.6250	0.626	0.6250	0.622	0.5000	0.496
0.125	0.5625	0.564	0.5625	0.562	0.5000	0.496
0.050	0.5250	0.520	0.5250	0.523	0.5000	0.503
0.015	0.5075	0.507	0.5075	0.504	0.5000	0.497
0.005	0.5025	0.500	0.5025	0.510	0.5000	0.498

^aThe D values are from Eq. (25).

^bThe $D_{\text{calc.}}$ values are from the computer simulations.

TABLE II. Rigid rod dimer rotational decay rates.

Radius a	Oseen		Rotne-Prager		No hydrodynamic interaction	
	α^a	$\alpha_{\text{calc.}}^b$	α	$\alpha_{\text{calc.}}$	α	$\alpha_{\text{calc.}}$
0.500	2.500	2.49	2.250	2.24	4.000	4.10
0.250	3.250	3.18	3.219	3.27	4.000	4.10
0.125	3.625	3.58	3.621	3.66	4.000	4.08
0.050	3.850	3.87	3.850	3.91	4.000	4.09
0.015	3.955	3.94	3.955	3.97	4.000	3.95
0.005	3.985	3.98	3.985	4.07	4.000	4.02

^aThe α values are from Eq. (25).

^bThe $\alpha_{\text{calc.}}$ values are from the computer simulations.

a negligible effect on D and α and they approach the "no hydrodynamic interaction" values. However, as the subunit radius is increased relative to the separation distance, the effects of the hydrodynamic interaction became apparent.

The hydrodynamic interaction increases the translational diffusion coefficient. The maximum value is $D = 0.75$ and it occurs when the two subunit spheres are in contact ($a = 0.5$). Both the Oseen and the Rotne-Prager approximations give the same result for the dimer translational diffusion coefficient.

In contrast to the effect on the translational diffusion coefficient, the hydrodynamic interaction decreases the rotational decay rate. Again, the maximum change occurs when the subunit spheres are in contact. In this configuration the Oseen tensor approximation yields a value of $\alpha = 2.5$ and the Rotne-Prager approximation yields a value of $\alpha = 2.25$. When the subunit radius is less than 0.1, the values of α obtained from the two approximations are essentially equivalent.

B. Harmonic dimer simulations

The harmonic dimer calculations paralleled those conducted on the rigid rod systems. Six harmonic dimer systems were studied with the subunit radius a varied from 0.5 to 0.005. In each simulation the potential width parameter was $\delta = 0.1$, the time step was $\Delta t = 0.00125$, and the total number of steps in the run was 10 000.

A difficulty arose for the system with $a = 0.5$. At this subunit radius the harmonic potential allows the two subunit spheres to move slightly "inside" each other so that the separation distance between the two spheres can be less than 1. When the separation distance is less than 0.75, the longitudinal element of the Oseen tensor exceeds the maximum allowable value of 1. In order to prevent this situation the potential width was reduced to $\delta = 0.05$ for this system. The time step was also decreased to $\Delta t = 0.0003$.

The translational diffusion coefficient and rotational decay rate were calculated for each system using Eqs. (23) and (24), respectively. The results for the harmonic systems were in agreement with those for the analogous rigid rod systems to within the accuracy of the calculations.

TABLE III. Harmonic dimer mean and mean square separation distances ($l = 1$, $a = 0.25$, $\delta = 0.1$).

	Eq. (26)	Computer simulation ^a	
		$\Delta t = 0.00125$	$\Delta t = 0.00025$
$\langle r \rangle$	1.020	1.019	1.020
$\langle r^2 \rangle$	1.050	1.050	1.050
Δr	0.098	0.1035	0.1006

^aThe Oseen tensor approximation was used in these calculations, which were run for 100 000 time steps.

The equilibrium properties of a Brownian particle system defined by the Fokker-Planck equation [Eq. (2)] [or by the equivalent Langevin equation (12)] are not affected by the hydrodynamic interaction. This is readily seen by noting that the steady state solution of the Fokker-Planck equation is the Boltzmann distribution function and is independent of the hydrodynamic tensor D_{ij} . In these computer experiments the mean and mean square separation distances between the two subunit spheres were calculated. The analytic values of $\langle r \rangle$ and $\langle r^2 \rangle$ to second order in δ are

$$\begin{aligned}\langle r \rangle &= l(1 + 2\delta^2/l^2 + \dots), \\ \langle r^2 \rangle &= l^2(1 + 5\delta^2/l^2 + \dots), \\ \Delta r &= (\langle r^2 \rangle - \langle r \rangle^2)^{1/2} = \delta(1 - 2\delta^2/l^2 + \dots).\end{aligned}\quad (26)$$

The values of $\langle r \rangle$ and $\langle r^2 \rangle$ obtained from the computer simulations were in good agreement with the analytic values of Eq. (26). The results from two simulations are compared with the analytic values in Table III. In the first experiment a time step of $\Delta t = 0.00125$ was used, while in the second a value of $\Delta t = 0.00025$ was used. Both simulations were run for 100 000 time steps. The simulation values of Δr are seen to be slightly larger than the analytical values ($\sim 6\%$ when $\Delta t = 0.00125$ and $\sim 3\%$ when $\Delta t = 0.00025$). The slight increase in Δr appears to be systematic and roughly proportional to the square root of the time step. It is probably a result of using a first order approximation to the force term in the displacement equation [Eq. (15)], where the integral of $\mathbf{F}(t)$ over time is approximated by $\mathbf{F}(t) \cdot \Delta t$ and $\mathbf{F}(t)$ is taken to be constant during the time step.

C. Harmonic trimer simulations

Three trimer systems were studied with subunit radii of $a = 0.5$, 0.25 , and 0.05 and a potential width of $\delta = 0.1$. A time step of $\Delta t = 0.00125$ was used and the simulations were run for 240 000 time steps. As was the case for the harmonic dimer, a problem arose with the Oseen tensor calculations when $a = 0.5$; however, the situation is even more restrictive for the trimer. For example, when the trimer is in a straight line configuration, a real solution to Eq. (17) does not exist for $a < 0.89$, while a could be as small as 0.75 for the dimer. To overcome this difficulty the hydrodynamic tensors were modified to be independent of the separation distance r when $r < 1$. The modified hydrodynamic tensor between two spheres separated by a distance less than one is therefore

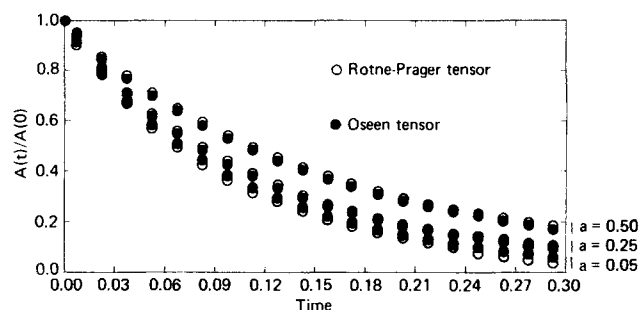


FIG. 2. The zero adjusted autocorrelation function $A(t)$ for the trimer simulations using the Oseen and Rotne-Prager approximations. The average value of $A(0)$ is 0.225.

$$D_{ij} = \frac{kT}{16\pi\eta a} \left(\bar{I} + \frac{\bar{r}\bar{r}}{r^2} \right) \quad (27)$$

in the Oseen calculations and

$$D_{ij} = \frac{kT}{16\pi\eta a} \left(\frac{7}{6} \bar{I} + \frac{1}{2} \frac{\bar{r}\bar{r}}{r^2} \right) \quad (28)$$

in the Rotne-Prager calculations. The gradient of the diffusion tensor is no longer equal to zero when $r < 1$, so this term must be included in the displacement equation as shown in Eq. (15).

The trimer translational diffusion coefficient was calculated using Eq. (23) and the results are shown in Table IV. The hydrodynamic interaction increases the diffusion coefficient. The increase becomes quite large as the subunit radii increase in size relative to the separation distance. At the maximum radius of 0.5 the diffusion coefficient with hydrodynamic interaction is nearly twice as large as the value obtained with no hydrodynamics.

Figure 1 shows the angle θ formed by the three subunit centers. The rate of change in θ was studied by calculating the zero adjusted autocorrelation function of $\cos\theta(t)$:

$$A(t) = \langle \cos\theta(t) \cdot \cos\theta(0) \rangle - \langle \cos\theta \rangle^2. \quad (29)$$

The autocorrelation results using the Oseen and Rotne-Prager approximations are shown in Fig. 2, where the curves are seen to relax to zero in a manner which is slower than exponential. The two hydrodynamic approximations give nearly the same result, the difference being within the statistical accuracy of the calculations. In the absence of hydrodynamic interaction the autocorrelation function $A(t)$ is nearly equal to the data shown in Fig. 2 for $a = 0.05$. Consequently, the effect of the hydrodynamic interaction is to slow the decay rate of $A(t)$.

TABLE IV. Harmonic trimer diffusion coefficients D .

Radius	Oseen	Rotne-Prager	No hydrodynamic interaction
0.50	0.619	0.621	0.332
0.25	0.482	0.483	0.333
0.05	0.365	0.364	0.334

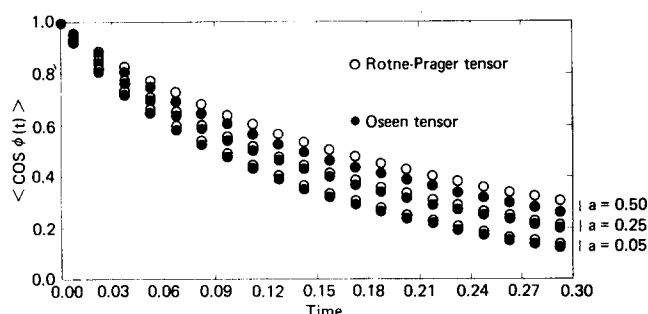


FIG. 3. The average value of $\cos\phi(t)$ for the trimer simulations using the Oseen and Rotne-Prager approximations.

The equilibrium values of $\cos\theta$ within $\pm 3\%$ were found to be $\langle\cos\theta\rangle = -0.18$ and $\langle\cos^2\theta\rangle = 0.258$, so that $A(0) = 0.225$. These properties for the analogous rigid rod trimer are $\langle\cos\theta\rangle = -0.25$, $\langle\cos^2\theta\rangle = 0.25$, and $A(0) = 0.1875$ and the minimum angle θ is 60° . Smaller angles (as small as 45°) are allowed with the harmonic potential with $\delta = 0.1$, resulting in a larger value of $A(0)$.

Movement of the plane defined by the three subunit centers can be studied by observing the change in direction of a unit vector perpendicular to the plane \hat{r}_1 . The angle ϕ formed by the initial direction of $\hat{r}_1(0)$ and a later direction can be calculated from the relationship

$$\cos\phi(t) = \hat{r}_1(0) \cdot \hat{r}_1(t). \quad (30)$$

The average value of $\cos\phi(t)$ was calculated and the Oseen and Rotne-Prager results are shown in Fig. 3. The behavior of $\langle\cos\phi(t)\rangle$ is similar to that of $A(t)$ in that it relaxes to zero in a manner which is slower than exponential. The effect of the hydrodynamic interaction on $\langle\cos\phi(t)\rangle$ is also the same as it is on $A(t)$, namely, it slows the decay rate of $\langle\cos\phi(t)\rangle$. The Rotne-Prager decay rate is slightly smaller than the Oseen decay rate and this effect is most pronounced when the spheres are in contact ($a = 0.5$).

VI. CONCLUSION

The results presented in the previous section demonstrates the importance of including hydrodynamic interactions in a dynamic simulation of many-particle Brownian systems. The hydrodynamic interaction is a long-range effect and influences the dynamics of even dilute solutions.^{17,27,28} Moreover, the hydrodynamic interaction profoundly influences the dynamics of diffusional encounters in solution²⁹⁻³³ and the description of the transport properties of multisubunit structures in terms of subunit frictional coefficients.³⁴⁻³⁸ Computer simulations should be useful for studying certain aspects of protein folding (e.g., the diffusion-collision model of Karplus and Weaver³⁹), particle coagulation, and other biochemical processes.

The role of hydrodynamic interactions in the dynamical properties of polymer solutions has long been appreciated,^{21,40,41} but simulations of polymer dynamics which incorporate these interactions have not been attempted. This is perhaps due in part to the appearance

of the square root of the diffusion tensor in the Langevin equations given by Lax¹⁹ and Zwanzig²⁰; this factor makes simulations based directly on the Langevin equations computationally very difficult. The methods described in this paper should make such simulations possible.

ACKNOWLEDGMENTS

The authors are grateful to Robert Nyholm and Liena Boone for carrying out the computer calculations. J. A. M. thanks Professor Peter Wolynes for helpful discussions and the N.I.H. for postdoctoral fellowship (1 F32 GM05717-01A1). The idea for this study was conceived during the 1976 CECAM workshop on models for protein dynamics (Orsay, France). This work was performed under the auspices of the U. S. Department of Energy by the Lawrence Livermore Laboratory under contract number W-7405-ENG-48.

- ¹A. Einstein, Ann. Phys. (Leipzig) 17, 549 (1905) [English translation reprinted in *Albert Einstein, Investigations on the Theory of Brownian Movement*, edited by R. Furth (Dover, New York, 1956)].
- ²M. V. Smoluchowski, Ann. Phys. (Leipzig) 21, 756 (1966).
- ³M. V. Smoluchowski, Ann. Phys. (Leipzig) 48, 1103 (1915).
- ⁴P. Langevin, C. Acad. Sci. 146, 530 (1908).
- ⁵A. D. Fokker, Dissertation, Leiden (1913).
- ⁶A. D. Fokker, Ann. Phys. (Leipzig) 43, 812 (1914).
- ⁷M. Planck, Sitzungsber. Preuss. Akad. Wiss. Phys. Math. Kl. 23, 324 (1917).
- ⁸O. Klein, Ark. Mat. Astron. Fys. 16, 5 (1922).
- ⁹H. A. Kramers, Physica (The Hague) 7, 284 (1940).
- ¹⁰G. E. Uhlenbeck and L. S. Ornstein, Phys. Rev. 36, 823 (1930) [reprinted in *Selected Papers on Noise and Stochastic Processes*, edited by N. Wax (Dover, New York, 1959)].
- ¹¹S. Chandrasekhar, Rev. Mod. Phys. 15, 1 (1943) [reprinted in *Selected Papers on Noise and Stochastic Processes*, edited by N. Wax (Dover, New York, 1954)].
- ¹²J. L. Lebowitz and E. Rubin, Phys. Rev. 131, 2381 (1963).
- ¹³J. L. Lebowitz and P. Resibois, Phys. Rev. Sect. A 139, 1001 (1965).
- ¹⁴P. Mazur and I. Oppenheim, J. Phys. Soc. Jpn. Suppl. 26, 35 (1969).
- ¹⁵J. Albers, J. M. Deutch, and I. Oppenheim, J. Chem. Phys. 54, 3541 (1971).
- ¹⁶R. M. Mazo, J. Stat. Phys. 1, 559 (1969).
- ¹⁷J. M. Deutch and I. Oppenheim, J. Chem. Phys. 54, 3547 (1971).
- ¹⁸T. J. Murphy and J. L. Aguirre, J. Chem. Phys. 57, 2098 (1972).
- ¹⁹M. Lax, Rev. Mod. Phys. 38, 541 (1966).
- ²⁰R. Zwanzig, Adv. Chem. Phys. 15, 325 (1969).
- ²¹H. Yamakawa, *Modern Theory of Polymer Solutions* (Harper and Row, New York, 1971).
- ²²J. Rotne and S. Prager, J. Chem. Phys. 50, 4831 (1969).
- ²³G. Wilemski, J. Stat. Phys. 14, 153 (1976).
- ²⁴D. L. Ermak and H. Buckholtz, J. Comp. Phys. (submitted for publication).
- ²⁵International Mathematical and Statistical Libraries, Inc., IMSL Library 3 Reference Manual, IMSL LIB3-0005, (Houston, TX, November 1975).
- ²⁶J. P. Ryckaert, G. Ciccoli, and H. J. C. Berendsen, J. Comp. Phys. 23, 327 (1977).
- ²⁷G. K. Batchelor, J. Fluid Mech. 74, 1 (1976).
- ²⁸P. G. Wolynes and J. M. Deutch, J. Chem. Phys. 67, 733 (1977).
- ²⁹H. L. Friedman, J. Chem. Phys. 70, 3931 (1966).
- ³⁰J. M. Deutch and B. U. Felderhof, J. Chem. Phys. 59, 1669 (1973).

- ³¹E. P. Honig, G. J. Roeberson, and P. H. Wiersema, J. Colloid Interface Sci. **36**, 97 (1971).
- ³²P. G. Wolynes and J. M. Deutch, J. Chem. Phys. **65**, 450 (1976).
- ³³P. G. Wolynes and J. A. McCammon, Macromolecules **10**, 86 (1977).
- ³⁴J. G. Kirkwood and J. Riseman, J. Chem. Phys. **16**, 565 (1948).
- ³⁵V. Bloomfield, W. O. Dalton, and K. E. Van Holde, Biopolymers **5**, 135, 149 (1967).
- ³⁶P. Debye and A. M. Bueche, J. Chem. Phys. **16**, 573 (1948).
- ³⁷B. U. Felderhof and J. M. Deutch, J. Chem. Phys. **62**, 2391 (1975).
- ³⁸J. A. McCammon, J. M. Deutch, and B. U. Felderhof, Biopolymers **14**, 2613 (1975).
- ³⁹M. Karplus and D. L. Weaver, Nature (London) **260**, 404 (1976).
- ⁴⁰M. Bixon, Ann. Rev. Phys. Chem. **27**, 65 (1976).
- ⁴¹W. H. Stockmayer, in *Molecular Fluids*, edited by R. Balian and G. Weill (Gordon and Breach, New York, 1976).